

## **[Chapter 2: Experimental Techniques and Characterization Methods]**

---

### **2.1 Experimental Techniques**

The synthesis of a good quality sample is one of the most important factors for obtaining desired physical properties of particular material and has been an area of increasing interest during recent years. Therefore, the selection of the type of synthesis technique for synthesizing the sample is a major task. Discovery of new phenomenon arises when the size of the resulting material and fundamental interaction distance both are of the same order which also serves as a guide for the development of leading cutting-edge technologies. The synthesis of the polycrystalline bulk manganite based materials can be classified into two main categories such as solid state reaction route and chemical method comprising sol-gel technique, co-precipitation technique, etc. [1-3]. Due to the simplicity of the planetary ball milling and sol-gel synthesis methods, all polycrystalline materials studied under present study have been synthesized using these methods. In order to develop a single-phase sample, the reaction conditions such as time, temperature, pH etc., during the synthesis are very important.

Each synthesis process has its own advantages and disadvantages based on several factors. Here, we have briefly discussed the planetary ball milling and the sol-gel route methods for preparing the nanoscale LSMFO particles.

#### **2.1.1 Planetary Ball Milling Method**

The poly-crystalline samples studied in the present work have been synthesized using the planetary ball milling method classified under solid state reaction method [4]. This is one of the most familiar methods for synthesizing the inorganic solids at elevated temperatures. If the entire constituents taking part in the reaction are in solid phase, the method is called the conventional ceramic method. As the name proposes, the solid forms of the constituents are allowed to react at high temperatures for a certain time which is generally attained by resistance heating. The general

## **[Chapter 2: Experimental Techniques and Characterization Methods]**

---

procedure involved in solid-state reaction technique for producing mixed valent manganite oxides is described. The planetary ball milling method has been considered as a better tool for preparing the number of advanced materials. Fig. 2.1 shows the schematic diagram of planetary ball milling set up. In any solid state route, the thermodynamic factor which involves change in free energy and kinetic energy involved in the route during the reaction are important.

The constituent materials for preparing the desired samples were ultrapure powders of carbonates, oxides, nitrides, etc., (~99.99% pure AR). These powders were pre-heated for fixed time duration and temperature in order to make them moisture free and indeseired proportion.

In the ball milling method, for the reaction to take place homogeneously, it is very important to mix and grind the oxide powders thoroughly for sufficient time. The obtained homogeneous distributed powder of desired stoichiometric ratio is put in a vital together with zirconia hardened balls in specific ball to powder ratio. The dry milling of the powders at required revolution per minute (rpm) is employed to mix the initial materials for obtaining the nanosize crystals, which is mandatory for obtaining the close contact among the atoms and for the formation of the desired material. After ball milling the samples, CO<sub>2</sub> is released from the mixture during the first calcinations and after the first heating. The samples are further heated at atmospheric conditions for obtaining samples with pure phase. To further release the residual CO<sub>2</sub>, before final sintering of the samples, the obtained fine black powder is reground and pressed into cylindrical pellets and sintered for longer period of time at high temperature. Many intermediate grindings are required for getting relevant phase formation and phase purity. The ball milling method is found to be the most suitable for synthesizing reproducible samples of colossal magnetoresistance materials (CMR).

## [Chapter 2: Experimental Techniques and Characterization Methods]

---

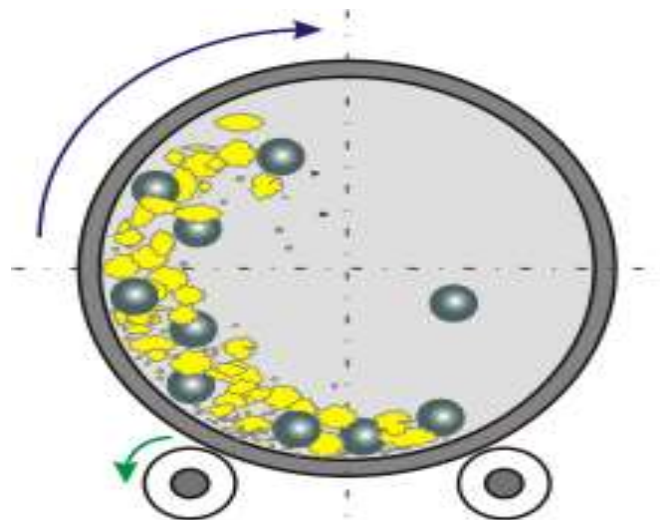


**Fig. 2.1:** Schematic diagram of ball milling method.

## [Chapter 2: Experimental Techniques and Characterization Methods]

---

### 2.1.2 Sol-Gel Method

The sol-gel route is an important method from the group of wet chemical route for synthesizing the oxide samples due to sample homogeneity and required lower sintering temperature. The sol-gel method is most conventional chemical route-based method for synthesizing the samples at large scale. The samples under the present study are also prepared by this technique. Various synthesis parameters such as sintering temperature and time, applied pressure at the time of palletizing the sample and grinding time are important during this process. Fig. 2.2 presents the schematic diagram of magnetic stirrer used in the sol-gel technique.

In sol-gel technique generally the selection of the proper nitrate material with purity is important for getting the final powder. These final powdered samples are then dissolved into distilled water and are kept in the hot plate of the magnetic stirrer so that the gel form of the homogeneous mixture is obtained. This gel is then dried at low temperature. The final grey powder obtained after drying procedure is grinded and calcinated at different temperatures to get the desired phase.



**Fig. 2.2:** Magnetic Stirrer set-up.

## **[Chapter 2: Experimental Techniques and Characterization Methods]**

---

### **2.2 Characterization Methods**

In experimental research, the characterization of the synthesized sample is the second most important step. In addition, the proper characterization techniques reveal information related to physical and chemical properties of given samples. There are various characterization techniques available for exploring the mechanism/phenomena related to the morphology of a material. Different techniques have various advantages and disadvantages and thus they complement each other.

In order to investigate the relationship of prepared samples with their structural properties, the characterization techniques like X-ray Diffraction (XRD) for structural properties, Raman Spectroscopy for vibrational properties, Field emission scanning electron microscopy (FE-SEM) for surface morphology, Energy Dispersive Analysis of X-ray (EDAX) for elemental studies and Vibrating Sample Magnetometer (VSM) for the study of magnetic properties are utilized. The following sections give a brief description about the various characterization tools mentioned above sequentially.

#### **2.2.1 X-ray Diffraction (XRD)**

In order to determine the proper phase and complete morphology of a material, it is essential to study its structural properties. The structural properties of any materials are closely related to the chemical characteristics of the constituent particles of the material and thus form the foundation on which detailed physical understanding is built. Powder XRD is the most commonly used X-ray diffraction technique for characterizing polycrystalline bulk materials by finding their crystal structure, atomic spacing and unit cell dimensions [5, 6]. The term 'powder' used in powder diffraction itself suggests that the material under study is in the powder form with randomly aligned fine grains of the crystalline material.

## [Chapter 2: Experimental Techniques and Characterization Methods]

---

X-ray diffraction (XRD) is a non-destructive tool for analyzing the properties of all kinds of matter ranging from fluids, to powders and crystals. This technique works under the principle of X-ray (or neutron) diffraction. The samples are usually in powder form or microcrystalline, where ideally every possible crystalline orientation is represented equally. Diffraction of X-ray occurs when there is a constructive interference between the monochromatic beam of X-rays and the crystalline sample. XRD technique offers varieties of information concerning the physical and electronic structure of crystalline and non-crystalline materials in a different conditions and environments [7]. For diffraction applications, X-rays with extremely short wavelengths (wavelength in the vicinity of  $1\text{\AA}$ ) are used. Thus, the wavelength of the X-ray beam used is of the same order of magnitude as that of the lattice constants of crystal which makes them suitable for the investigation of crystal structures [8, 9].

The XRD pattern obtained for substance is, like a fingerprint of the substance. While passing through a crystal, X-rays based on their wavelength, orientation and structure of the crystals are diffracted by the atoms at specific angles. X-rays are predominantly diffracted (scattered) by electrons and analysis of the diffraction angles produces an electron density map of the crystal. These values depend on the wavelength of the X-ray and lattice constants of the crystal, and consequently it seems reasonable to use concept of physical optics to understand the selective reflectivity in terms of interference effects. In this way, the X-rays basically scatter or interact with the electrons of the atoms and hence carry information about the electron distribution in materials.

When the photons of the X-ray collide with electrons, some of the photons from the incident beam get deviated from the incident direction. Diffracted X-ray waves from atoms can interfere with each other and the resultant intensity distribution is strongly modulated by this

## [Chapter 2: Experimental Techniques and Characterization Methods]

---

interaction. The peaks in the X-ray diffraction pattern are directly related to the inter-atomic distances. The incoming X-ray beam of wavelength  $\lambda$  will undergo scattering process followed by constructive interference only when the incident X-ray beam falls and passes through the adjacent lattice planes at specific angles ' $\theta$ ', that satisfies the well-known Bragg's condition for diffraction originally developed by Bragg in 1915. The set of lattice planes of a crystal can be represented as the horizontal lines resulting from the periodic order of atoms. In other words, for a given set of lattice planes with an inter plane distance ' $d$ ', the condition for the occurrence of the diffraction (peak) as per Bragg's law can be written as,

$$n\lambda = 2d\sin\theta \quad (1)$$

Where  $d$  = inter planar distance,  $n$  = order of reflection (integer value),  $\lambda$  = wave length of X-rays,  $\theta$  = angle between incident/reflected beam and particular crystal planes under consideration.

Bragg's law in the simplest sense gives the condition for constructive interference for X-rays incident on a set of lattice planes. The process of diffraction is described in terms of incident and diffracted (reflected) rays, each making an angle  $\theta$  with a fixed crystal plane. Reflection occurs from the planes at an angle  $\theta$  with respect to the incident beam and generates a reflected beam at an angle  $2\theta$  from the incident beam. The possible " $d$ " spacing defined by the Miller indices, indices  $h, k, l$  are determined by the alignment of the unit cell. Thus, the possible  $2\theta$  values where we can have reflections are determined by the unit cell dimensions. It is noteworthy that the law does not refer to the composition of the basis atoms associated with every lattice point. It was observed in 1918 by Scherrer that the crystallite of small size gives rise to line broadening in diffraction spectra. The Debye-Scherrer formula is given,

$$D = 0.9\lambda / \beta \cos\theta \quad (2)$$

## [Chapter 2: Experimental Techniques and Characterization Methods]

---

Where  $\lambda$  is the wavelength of X-ray,  $\beta$  is line broadening at full width at half maximum (FWHM) and  $\theta$  is the diffraction angle. The details of the basic principle of XRD techniques and description can be found in Refs. [8, 10-12]. The position and the intensity of the peaks in typical powder diffraction spectrum consisting a plot of reflected intensities versus diffraction angle ( $2\theta$ ) are used to determine the underlying structure of the material. The powder method is used to determine the value of the lattice parameters accurately. Lattice parameters are the magnitude of the unit vectors  $\vec{a}$ ,  $\vec{b}$ , and  $\vec{c}$ , which define the fundamental unit cell for the crystal. Therefore, the intensities depend on what kind of atoms we have and where in the unit cell they are located.

Let us consider an incident X-ray beam interacting with the atoms ordered in a periodic manner and the typical X-ray diffractometer used for the analysis of the samples as shown in Figs. 2.3 and 2.4 respectively.

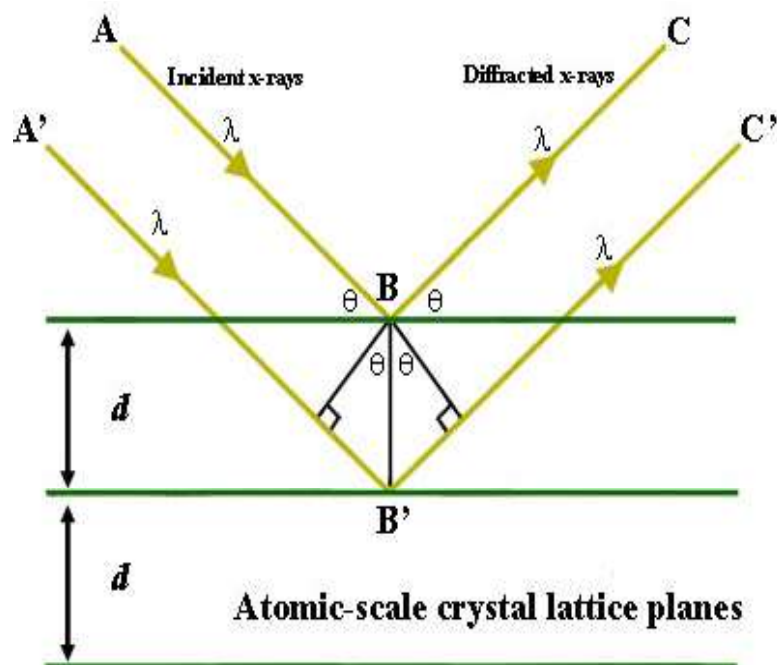


**Fig. 2.3:** Schematic diagram depicting the Bragg's law of X-ray diffraction. The symbols used in the schematic have their usual meaning.

## [Chapter 2: Experimental Techniques and Characterization Methods]

---

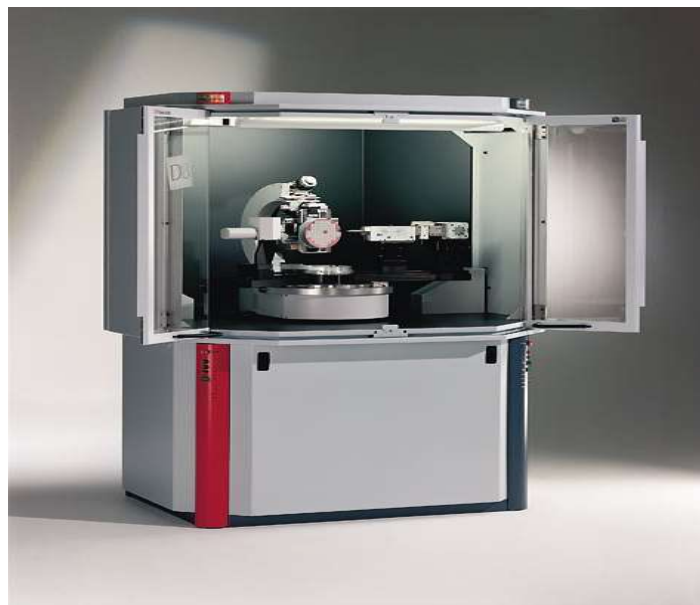


**Fig. 2.4:** Powder XRD apparatus set-up.

The XRD pattern of all samples in the present study was recorded by Philips Pro X'Pert PANalytical Pro using Cu-K $\alpha$  radiation at room temperature for structural identification. The structural studies of the samples are performed by Rietveld refinement method. The Rietveld analysis is described below.

### 2.2.2 Rietveld Analysis

The Rietveld analysis is a refinement method for powder diffraction patterns originally proposed by Hago Rietveld to study the crystallographic, nuclear and magnetic structures of crystalline materials [13-15]. The Rietveld method refines user-selected parameters to minimize the difference between an experimental pattern (observed data) and a model based on the hypothesized crystal structure and instrumental parameters (calculated pattern). This approach uses a least square fitting method to refine a theoretical line until it matches the measured profile i.e. obtained XRD data from diffractometer. This technique was quite successful in analysis of diffraction of powder samples mainly due to its ability to deal reliably with strongly overlapping

## [Chapter 2: Experimental Techniques and Characterization Methods]

---

reflections [16]. There are six factors affecting the relative intensities of the diffraction lines on a powder pattern such as, polarization factor, structure factor, multiplicity factor, Lorentz factor, absorption factor and temperature factor.

The parameters refined using Rietveld refinement method fall into mainly three classes: peak shape function, profile parameters and atomic structural parameters. The peak shapes depend on both sample (e.g. domain size, stress/strain, defects) as well as the instrument parameters (e.g. radiation source, geometry, slit sizes) which vary as a function of  $2\theta$ . The lattice parameters, shape of Bragg peaks and the width of the Bragg peaks are generally called the profile parameters. The peak widths are actually smooth function of the scattering angle  $2\theta$ . The atomic position, occupancies of the atoms and thermal parameters are the structural parameters which describe the model [17]. The X-ray diffraction provides the information about the crystallographic structure while polarized neutron beams are used for studying the magnetic structure. The structure of a material is described with a large number of parameters representing the experimental set-up. These consist nine parameters such as wavelength, scale factor, zero point for  $2\theta$  and six parameters for a polynomial background. For the typical  $\text{LaMnO}_3$  ( $\text{ABO}_3$ ) type perovskite structure, most of the parameters have to be refined. The gradient for the weighted sum of squared difference between the calculated intensities and the measured intensities  $R_p$  can be determined relative to these parameters. The gradient is then used to change the parameters and this is repeated until a minimum in the  $M_p$  function is reached. The definition of  $R_p$  and the profile factors are described in FullProf manual and defined as,

$M_p$  is defined as

$$M_p = \sum_i w_i Y_{io} - Y_{ic} \quad (3)$$

## [Chapter 2: Experimental Techniques and Characterization Methods]

---

Where  $W_i$  is a weight function,  $Y_{i0}$  is the observed intensity at angular step  $i$ ,  $Y_{ic}$  is the corresponding calculated intensity. To control the quality of the refinement, several agreement factors can be calculated.

The profile factor:

$$R_p = 100 \frac{\sum_{i=1,n} |y_i - y_{c,i}|}{\sum_{i=1,n} y_i} \quad (4)$$

Weighted profile factor:

$$R_{wp} = 100 \left[ \frac{\sum_{i=1,n} w_i |y_i - y_{c,i}|^2}{\sum_{i=1,n} w_i y_i^2} \right]^{1/2} \quad (5)$$

Expected weighted profile factor:

$$R_{exp} = 100 \left[ \frac{n - p}{\sum_{i=1,n} w_i y_i^2} \right]^{1/2} \quad (6)$$

Bragg factor:

$$R_B = 100 \frac{\sum_h |I_{obs,h} - I_{cal,h}|}{\sum_h |I_{obs,h}|} \quad (7)$$

Crystallographic  $R_F$  factor:

$$R_F = 100 \frac{\sum_h |F_{obs,k'} - F_{cal,h}|}{\sum_h |F_{obs,h}|} \quad (8)$$

Goodness of fit indicator:

$$S = \frac{R_{wp}}{R_{exp}} \quad (9)$$

## [Chapter 2: Experimental Techniques and Characterization Methods]

---

Reduced chi- square:

$$\chi_v^2 = \left[ \frac{R_{wp}}{R_{exp}} \right]^2 = S^2 \quad (10)$$

The Rietveld refinements of the samples prepared in present work were made using FullProf program.

### 2.2.3 Scanning Electron Microscope (SEM)

The electrons are used as a probe to form an image of the specimen in the case of scanning electron microscopy. It is one of the most powerful and a productive method of microscopy has allowed researchers to examine a large variety of specimens [18, 19]. The SEM has many advantages over traditional microscopes. Most significant advantage is its large depth of field which allows major part of the specimen under focus at one time. The SEM which is a non-destructive technique also has much higher resolution to magnify closely spaced specimens much higher levels. The several advantages together with the clear images make scanning electron microscope one of the most useful instruments for examination and evaluation of materials. Fig 2.5 shows the schematic diagram of SEM apparatus.



**Fig. 2.5:** SEM apparatus set-up.

## [Chapter 2: Experimental Techniques and Characterization Methods]

---

### Working of SEM

Fig. 2.6 shows schematic diagram representing the working principle of Scanning Electron Microscope. As shown in the figure, a beam of electrons is produced at the head of the microscope by an electron gun. The electron beam is passed through an anode and then passed through a magnetic condensing lens. The function of magnetic condensing lens is to compress the electron beam. A scanning coil is fixed between magnetic condensing lens and the specimen. The subsidiary electrons are collected by a scintillator and then transformed to the electrical signal. These signals are then sent to CRO via video amplifier. Every point on the specimen where accelerated electrons fall releases the signal in the form of electromagnetic radiation. While subsidiary and backscattered electrons (BSE) are composed by a detector the outcome signal is amplified and displayed on computer screen.

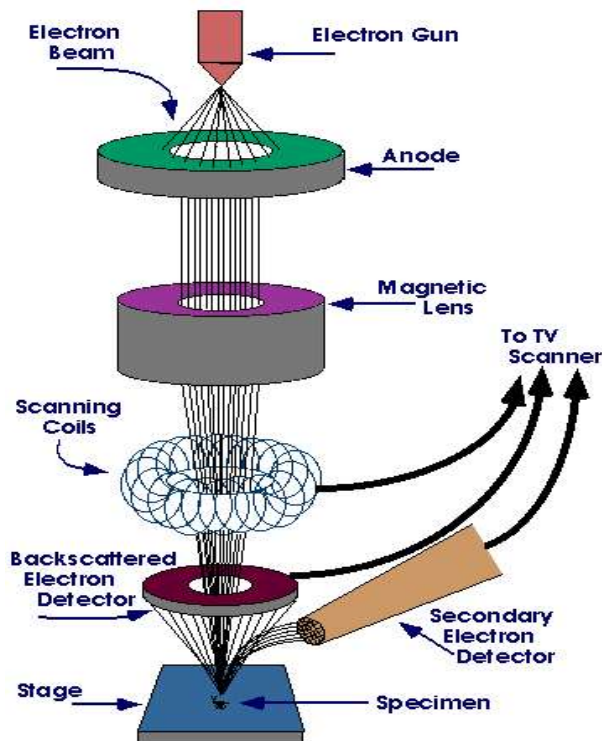


**Fig 2.6:** Schematic diagram depicting the working of a Scanning Electron Microscope.

## **[Chapter 2: Experimental Techniques and Characterization Methods]**

---

Scanning Electron Microscopy does not require much samples. For achieving better surface morphological and grain size information the surface of the sample may be cleaned and smoothed before it is used for scanning purpose.

### **2.2.4 Field Emission Scanning Electron Microscope (FE-SEM)**

Field Emission Scanning Electron Microscopy (FE-SEM) is an analytical technique used in material science for investigating the molecular surface structures and their electronic properties [20]. Invented by Erwin Wilhelm Müller in 1936, the FE-SEM was one of the first surface-analysis instruments with near-atomic resolution.

Microscopy techniques are used to produce real-space magnified images of a surface. In general, microscopy information concerns surface crystallography (i.e. how the atoms are arranged at the surface), surface morphology (i.e. the shape and size of topographic features making the surface) and surface composition (the elements and compounds the surface is composed of) [21].

The biggest difference between the FE-SEM and SEM lies in the electron generation system. As a source of electrons, the FE-SEM uses a field emission gun that provides extremely focused high and low-energy electron beams, which greatly improves spatial resolution and enables work to be carried out at very low potentials (0.02–5 kV). This helps to minimize the charging effect on non-conductive specimens and to avoid damage to electron beam sensitive samples. Another highly remarkable feature of FE-SEM is its use of in-lens detectors. These detectors, which are optimized to work at high resolution and very low acceleration potential, are fundamental parameters for getting the maximum performance from the equipment.

Field emission scanning electron microscope (FE-SEM) provides topographical and elemental information at magnification of 10X to 300,000X, with virtually unlimited depth of the

## [Chapter 2: Experimental Techniques and Characterization Methods]

---

field. Compared with the conventional scanning electron microscopy (SEM), the field emission SEM (FE-SEM) produces clearer and less electrostatically distorted images with spatial resolution three to six times better. An FE-SEM is a microscope that deals with electrons (particles with a negative charge) instead of the electromagnetic waves; i.e. light. The electrons are liberated by a field emission source. The object is scanned by electrons according to a zig-zag pattern. The FE-SEM used for characterizing the samples under the present work is shown in Fig. 2.7.



**Fig. 2.7:** FE-SEM used for characterization of the samples.

The electron beam is focused by the electro-magnetic lenses (condenser lens, scan coils, stigmator coils and objective lens) and the apertures in the column to a tiny sharp spot. Electrons are liberated from a field emission source and accelerated in a high electrical field gradient. Within the high vacuum column these so-called primary electrons are focused and deflected by electronic lenses to produce a narrow scan beam that bombards the object. As a result, secondary electrons are emitted from each spot on the object. The angle and velocity of these secondary electrons are related to the surface structure of the object. A detector catches the secondary electrons and produces an electronic signal. This signal is amplified and transformed to a video scan-image that can be seen on a monitor or to a digital image and saved for further process. The

## **[Chapter 2: Experimental Techniques and Characterization Methods]**

---

FE-SEM has many applications such as semiconductor device cross section analyses for gate widths, gate oxides, film thicknesses and construction details, advanced coating thickness and structure uniformity determination, small contamination feature geometry and elemental composition measurement. The FE-SEM also has the ability to examine smaller-area contamination spots at electron accelerating voltages compatible with energy dispersive spectroscopy (EDS).

### **2.2.5 Transmission Electron Microscope (TEM)**

The transmission electron microscopy (TEM) is a very powerful technique to study the size and size distribution of nanoparticle samples in material science. The first TEM was demonstrated in 1933 by Max Knoll and Ernst Ruska with resolution greater than that of light. The TEM operates on the same basic principles as the light microscope but uses electrons instead of light which are scattered while passing through a thin-section specimen of a material. A sophisticated system of electromagnetic lenses focuses the scattered electrons into an image or a diffraction pattern or a nanoanalytical spectrum depending on the mode of operation. It consists an electron gun to produce electrons and magnetic condensing lens to condense the electrons. It is also used to adjust the size of the electron that falls on to the specimen. The magnetic objective lens is used to block the high angle diffracted beam and the aperture is used to eliminate the diffracted beam (if any) and in turn increases the contrast of the image. The magnetic projector lens is placed above the fluorescent screen in order to achieve higher magnification. The image can be recorded by using a fluorescent (Phosphor) screen or Charged Coupled device (CCD).

### **Working of Transmission Electron Microscope**

Stream of electrons are produced by the electron gun and is allowed to fall over the specimen using the magnetic condensing lens. Based on the angle of incidence the beam is

## [Chapter 2: Experimental Techniques and Characterization Methods]

---

partially transmitted and partially diffracted. Both these beams are recombined at the Ewald sphere to form the image. The combined image is called the phase contrast image. In order to increase the intensity and the contrast of the image, an amplitude contrast has to be obtained which can be achieved only by using the transmitting beam and thus the diffracted beam can be eliminated. Now in order to eliminate the diffracted beam, the resultant beam is passed through the magnetic objective lens and the aperture. The working diagram of Transmission Electron Microscope is shown in Fig. 2.8. The aperture is adjusted in such a way that the diffracted image is eliminated. Thus, the final image obtained due to transmitted beam alone is passed through the projector lens for further magnification. This high contrast image is called Bright Field Image. Also, it has to be noted that the bright field image obtained is purely due to the elastic scattering (no energy change) i.e., due to transmitted beam alone. TEM is an impressive instrument with a number of advantages such as powerful magnification, potentially over one million times or more. It has a wide range of applications and can be utilized in a variety of different scientific, educational and industrial fields. TEMs are able to yield information of surface features, shape, size and structure.

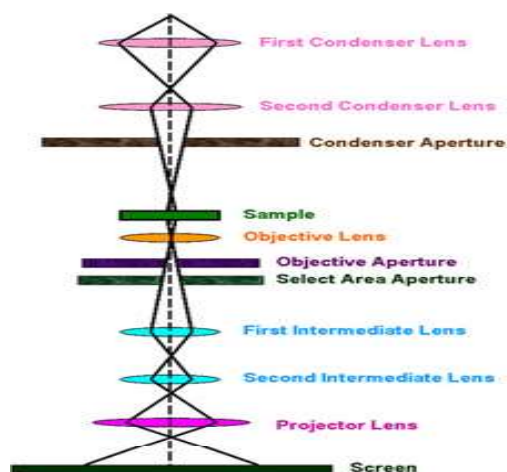


**Fig. 2.8:** Schematic diagram representing working of TEM.

## [Chapter 2: Experimental Techniques and Characterization Methods]

---

### 2.2.6 Energy Dispersive Analysis of X-ray (EDAX)

Energy Dispersive analysis of X-ray (EDAX) is an X-ray microanalysis technique that involves X-rays for studying the materials at very small scales, ranging from micro to atomic levels and being extensively used by scientific community. The X-ray microanalysis for the routine chemical analysis of small volumes is considered best despite of having many microanalytical techniques. EDAX is a powerful and easy technique to reveal the presence of elements in a particular specimen. In EDAX setup, the X-rays produced by each element after bombarding a sample with high energy electrons in an electron microscope are detected. The X-ray mapping process is used to collect the information about the elemental composition of a sample. The EDAX is useful due to the fact that the X-rays from each element bear a direct relationship with the concentration i.e. mass or atomic fraction of that element. Fig. 2.9 displays a schematic diagram of the EDAX setup.

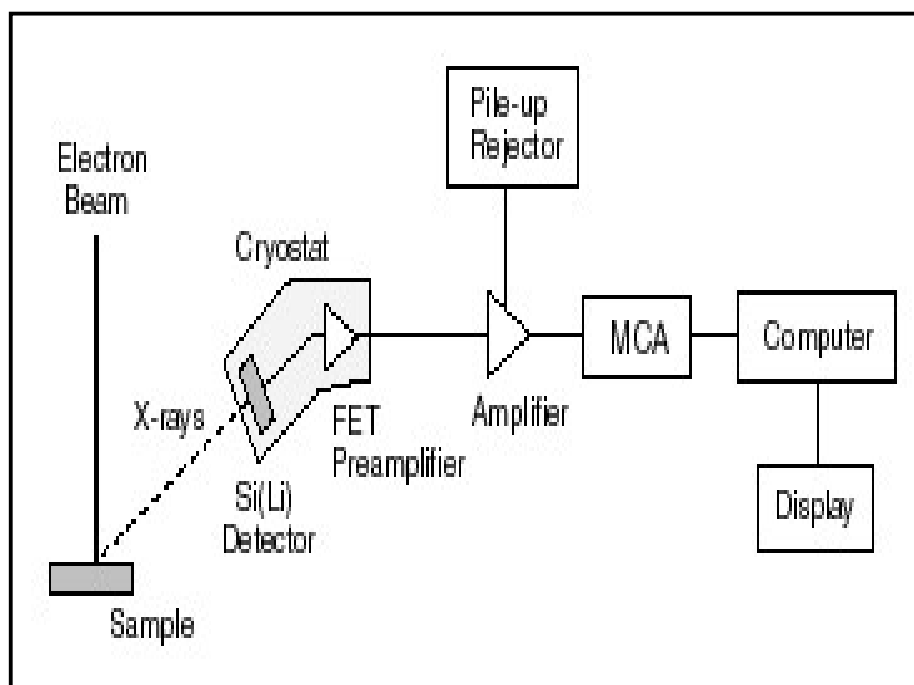


**Fig. 2.9:** Schematic representation of EDAX.

## [Chapter 2: Experimental Techniques and Characterization Methods]

---

### 2.2.7 Raman Spectroscopy

The Raman spectroscopy which is based on the Raman effect originally discovered by C.V. Raman in 1930 is the most common vibrational spectroscopic technique for assessing molecular dynamics and fingerprinting species based on inelastic scattering of a monochromatic source. When light scatters from an atom or crystal, most of the photons get scattered elastically and these scattered photons have the same energy and wavelength as that of the incident photons. However, a little fraction of light (approximately 1 in 10<sup>7</sup> photons) is scattered at optical frequencies dissimilar from and generally lower than the frequency of the incident photons. This phenomenon of inelastic scattering is known as Raman effect. Raman scattering takes place with a change in vibrational, rotational or electronic energy of the molecule.

When light in the form of electromagnetic radiation interacts with matter, the photons may be absorbed or scattered, or may not interact with the material at all and may simply pass through it. If the energy of an incident photon is proportional to the energy gap between the ground state and an excited state the molecule is promoted to the higher energy excited state after photon is absorbed. It is this change which is measured in an absorption spectroscopy. However, it is also possible for the photon to interact with the molecule and get scattered from it. The scattered beams of photons are observed by collecting light at an angle to the incident beam. In the case of Raman scattering efficiency is directly proportional to the fourth power of the frequency of the incident light.

To study the physics of the materials, the scattering experiments play major role as it helps to understand the spatial arrangement of the atoms. The Brillouin scattering which is scattering of light from low energy acoustic phonons is an influential tool for understanding the science behind the acoustic phonon and elasticity of the material. The study performed using

## [Chapter 2: Experimental Techniques and Characterization Methods]

elastic scattering provides information of the crystal structure, including the magnetic state of the crystal. Figs. 2.10 and 2.11 show the working and general experimental set up for obtaining Raman Spectra.

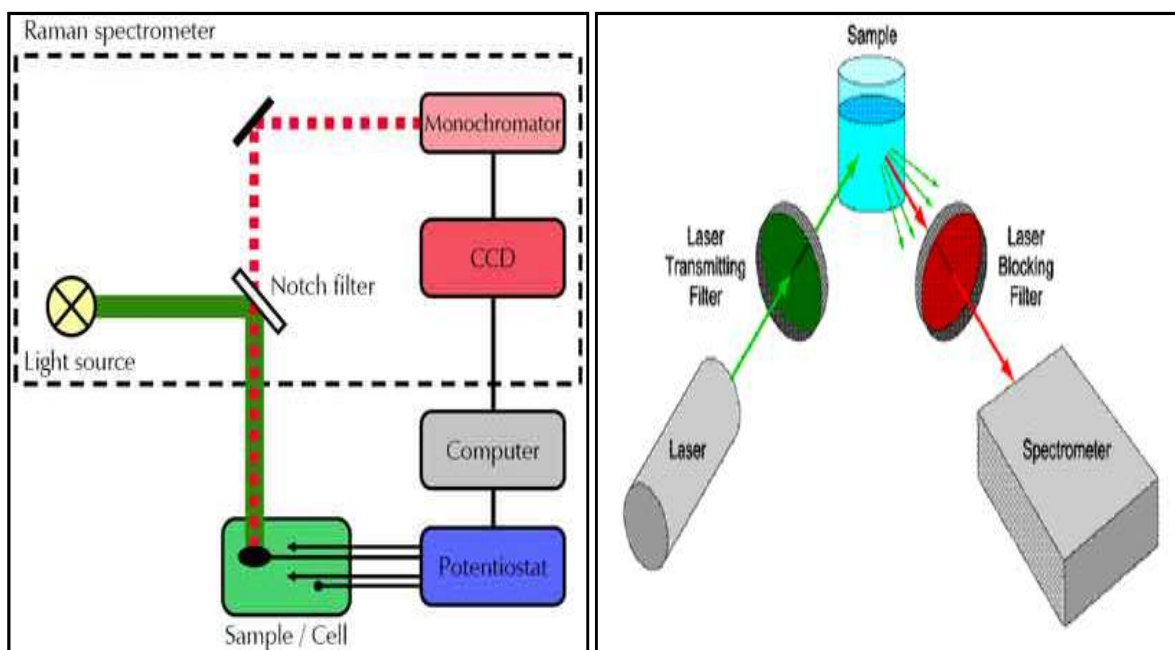


**Fig. 2.10:** Schematic diagram depicting the working of Raman Spectra.



**Fig. 2.11:** Instrument set-up of Raman Spectroscopy.

## [Chapter 2: Experimental Techniques and Characterization Methods]

---

### 2.2.8 Vibrating Sample Magnetometer (VSM)

The measurement of magnetic properties of any material is an important aspect mainly for understanding the mechanism of magnetic materials before fabricating the magnetic devices. The magnetic properties of the material are measured by Vibrating Sample Magnetometer (VSM) which was invented by Simon Foner at MIT Lincoln Laboratory in 1955 and reported in 1959 [22]. The study of magnetic properties of materials involves understanding of the electronic behavior in condensed matter and material science. The electrons show highly correlated behavior i.e. the conduction electrons depend on the presence or absence of neighbour electrons in varieties of inorganic compounds and alloys of transition metals. These electronic correlations result in changes in material properties like magnetism, superconductivity, metal-insulator transitions or heavy fermion behavior of conduction electrons. These behaviors are highly influenced by the Coulomb and exchange interactions among electrons. The working diagram of VSM is shown in Fig. 2.12.

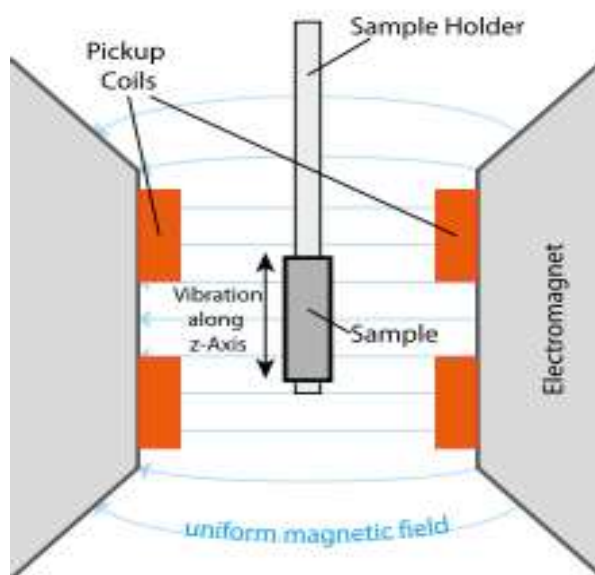


**Fig. 2.12:** Schematic diagram depicting the working of VSM.

## [Chapter 2: Experimental Techniques and Characterization Methods]

---



**Fig. 2.13:** PPMS Quantum Design set-up.

The basic working principle of a vibrating sample magnetometer (VSM) which provides information about the changing magnetic field is based on Faraday's Law of induction, which tells us that the modification in the magnetic field produces a measurable electric field. The sample to be studied is kept in a constant uniform magnetic field. Superconducting Quantum Interference Device (SQUID) magnetometers are classified within the flux methods of measuring magnetization of a sample. This is useful to measure the small magnetic fields in a most sensitive way. The electromagnet gets activated before the testing starts so if the sample is magnetic in nature, it will be magnetized and stronger magnetic field is produced. This results in magnetic field  $\vec{H}$  around the sample. The magnetization of the specimen can be analyzed due to vibration in the sample due to magnetization of sample as changes occur in relation with the time period of the movement. The changes in the magnetic flux prompt a voltage in the sensing coil proportional to the magnetization of the sample. A schematic diagram of VSM instruments is shown in Fig. 2.13.

## [Chapter 2: Experimental Techniques and Characterization Methods]

---

### 2.2.9 X-ray Photoemission Spectroscopy (XPS)

X-ray photoelectron spectroscopy (XPS) is a surface characterization technique that can analyze a sample to a depth of 2 to 5 nanometers (nm). It was developed by Nobel Laureate Kai Siegbahn in 1960s. The working diagram of XPS instrument is presented in Fig. 2.14. XPS reveals the presence of chemical elements at the surface and the nature of the chemical bond between elements. It can detect all elements except hydrogen and helium. It provides information about elemental composition with up to 0.1% sensitivity, chemical state information, thickness measurement of overlayers of up to 8 nm on a substrate, surface chemical imaging, thickness and depth-distribution of chemical species, depth profiling the Valence Band photoelectron Spectroscopy (VBS). This also provides information on the density of states in the valence band and electron work function.

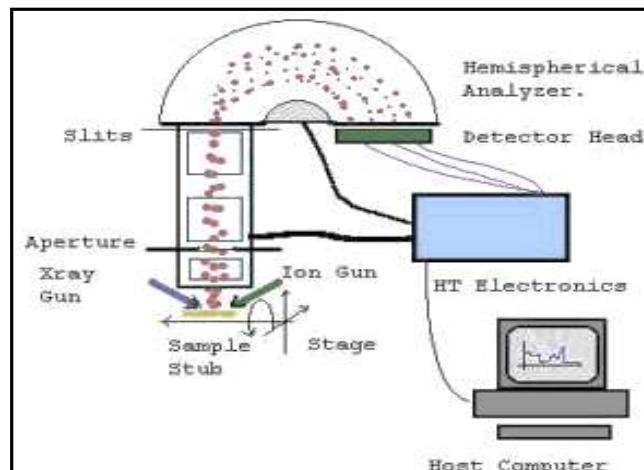


**Fig. 2.14:** XPS apparatus set-up.

A surface in this case is irradiated with X-rays (commonly Al  $K\alpha$  or Mg  $K\alpha$ ) in vacuum. When the X-ray photon hits and transfers its energy to a core-level electron, it is emitted from its initial state with a kinetic energy dependent on the incident X-ray and binding energy of the atomic orbital from which it is emitted. The energy and intensity of the emitted photoelectrons

## [Chapter 2: Experimental Techniques and Characterization Methods]

---

are analyzed to identify and determine the concentrations of the elements present. These photoelectrons originate from a depth of <10 nm therefore the information obtained is from within this depth.

### 2.2.10 Thermal Analysis

#### 2.2.10.1 Differential Scanning Calorimetry (DSC)

Thermal analysis is defined as “a series of techniques for measuring the temperature dependency of physical properties of a certain substance while varying the temperature of the substance according to a specific program.” The substance referred here includes reaction products. The physical properties include mass, temperature, enthalpy, dimension, dynamic characteristics etc. DSC is a thermo-analytical technique in which the difference in the amount of heat required to increase the temperature of a sample and reference is measured as a function of the temperature. The technique was developed by E. S. Watson and M. J. O'Neill in 1960 [23]. The differences in heat flow occur with the occurrence of two major events:

- 1) The heat capacity of the sample which increases with temperature (baseline)
- 2) Transitions that occur in the sample. Heat flow rate can be expressed in a variety of units and can be normalized for the weight of sample used [23].



**Fig. 2.15:** Set-up of Differential Scanning Calorimeter.

## [Chapter 2: Experimental Techniques and Characterization Methods]

---

A DSC consists of a cell connected with a gas inlet through which different gases are purged depending on the data required (see Fig. 2.15). Based on the DSC cells, there are two primary types: Heat flux which consists of a large single furnace acting as an infinite heat sink to provide or absorb heat from the sample. The advantages generally include a better baseline, sensitivity and sample–atmosphere interaction. Fig. 2.16 is a schematic of a heat flux DSC. The key components are the sample pan which is combined with the Reference pan. The dynamic sample chamber is the environment of the sample pan compartment and the purge gas. Nitrogen is the most common gas, but alternate inert gas is helium or argon. The heat flux DSC is based on the change in temperature  $\Delta T$  between the sample and reference and is indicated in Fig. 2.16.

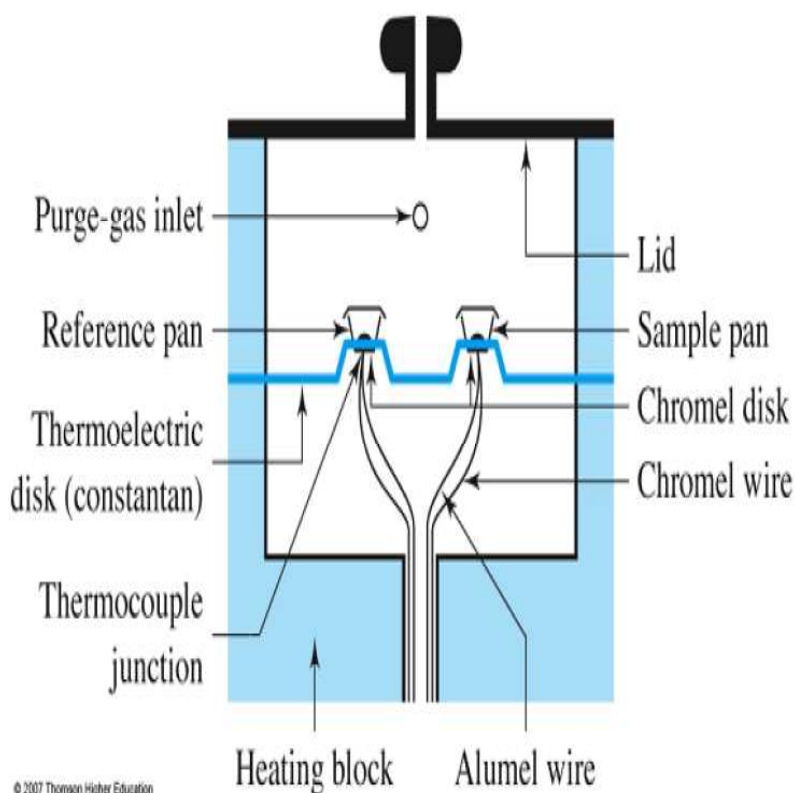


**Fig. 2.16:** Heat flux DSC cell cross section.

## [Chapter 2: Experimental Techniques and Characterization Methods]

---

Power compensation small individual furnaces use different amounts of power to maintain a constant  $\Delta T$  between sample and reference and the advantage here include faster heating and cooling, and better resolution as shown in Fig. 2.17. There are two individually separate chambers for sample and reference material with platinum heaters monitors the difference between the sample and reference. Platinum resistance thermometers track the temperature variations for the sample and reference cells. Holes in the compartment lids allow the purge gas to enter and contact the sample and reference. There are physical differences between the heat flux and power compensated thermal analysis. However, resulting fusion and crystallization temperatures are the same. The heat of transition is comparable quantitatively [23, 24].

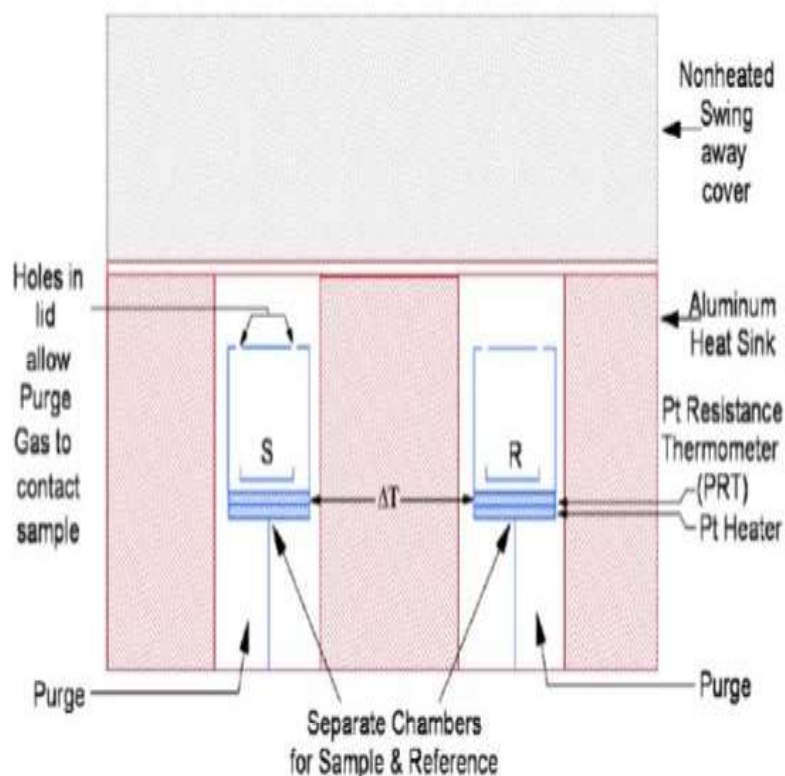


**Fig. 2.17:** Power Compensation DSC Cell Design.

## **[Chapter 2: Experimental Techniques and Characterization Methods]**

---

It is recommended that the sample to be used for DSC measurement should be thin and cover maximum bottom area of the pan. Samples in the form of cakes (as in case of polymers) must preferably be cut rather than crushed to obtain a thin sample. Crushing the sample, whether in crystalline form or a polymer, induces a stress, which can in turn affect the results. In most cases lids should always be used in order to more uniformly heat the sample and to keep the sample in contact with the bottom of the pan. DSC is used in studying the melting, crystallization, glass transition, oxidation and decomposition of pharmaceuticals. By selecting different parameters useful data such as the purity, polymorphic transitions can be obtained. A typical DSC curve could give glass transition temperature, melting temperature, crystallization temperature and decomposition temperatures [24-26].

The DSC is used to determine the transition temperature, heat of fusion of a crystal phase, the degree of crystallization, heat capacity, heat of formation and sample purity. The main application of DSC is in studying phase transitions such as melting point, glass transitions, or exothermic decompositions. These transitions involve energy changes or heat capacity changes that can be detected by DSC with great sensitivity [26].

### **2.2.10.2 Thermogravimetric Analysis (TGA)**

Thermogravimetric analysis or thermal gravimetric analysis (TGA) is a method of thermal analysis in which the mass of a sample is measured over time as the temperature changes [27]. The TGA measures the amount and the rate of weight change of a material with respect to temperature or time in controlled environments. The thermogravimetric analyzer is shown in the Fig. 2.18 (a) and (b). The TGA consists three major parts; a furnace such as microgram balance, an auto sampler and thermocouple. The furnace made of quartz can raise the temperature as high as 1000°C. The auto sampler helps to load the samples on to the microbalance. The

## [Chapter 2: Experimental Techniques and Characterization Methods]

---

thermocouple sits right above the sample. Care should be taken at all times that the thermocouple is not in touch with the sample which is in a platinum pan [28].

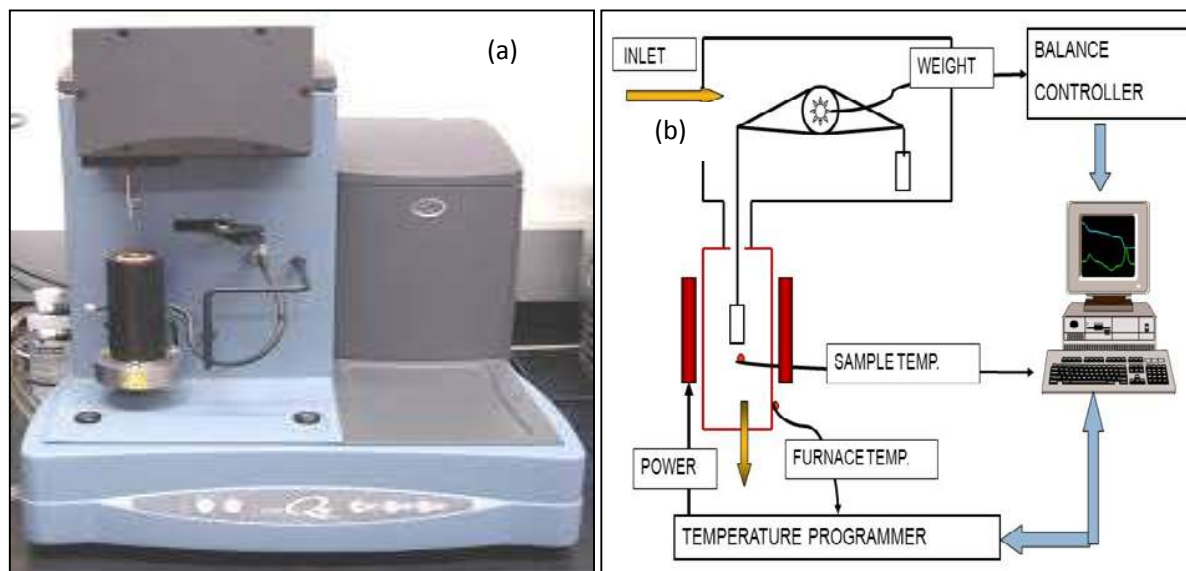


**Fig. 2.18:** (a) Thermogravimetric Analyzer (TGA) and (b) Instrumental set-up of the TGA Analyzer.

Sample preparation plays a significant role in obtaining good data. It is suggested that the maximizing the surface area of the sample in a TGA pan improves the resolution and reproducibility of weight loss temperatures. The sample weight affects the accuracy of weight loss measurements. Typically, 10-20 mg of sample is preferred in most of the applications. However, when sample is volatile, then 50-100 mg of sample is considered adequate. It is to be noted that most TGA instruments have baseline drift of  $\pm 0.025$  mg which is  $\pm 0.25\%$  of a 10 mg sample.

The most important experimental parameter of the TGA analysis is the heating rate. The samples are normally heated at the rate of 10 or 20°C/min. Lowering of heating rate improves resolution of overlapping weight losses. The technology advancement has made the analysis possible for variable heating rates to improve resolution by automatically reducing the heating

## **[Chapter 2: Experimental Techniques and Characterization Methods]**

---

rate during periods of weight loss. The nitrogen due to its inert nature is the most common gas used to purge samples in TGA. Air is known to improve resolution because of a difference in the oxidative stability of components in the sample. Vacuum may also be used in the case of volatile samples. There are generally two limitations of TGA for analyzing the materials:

- 1) The decomposition of sample in the case of multiple component system.
- 2) Though TGA is quantitative method, it cannot identify the decomposition products.

For this TGA coupled with mass spectrometer or FTIR can be used.

TGA can be used to know the composition of multi-component system, thermal stability of materials, oxidative stability of materials, decomposition kinetics of materials, the effect of reactive or corrosive atmosphere on materials, moisture and volatiles contents on materials and sublimation behavior of the various substances. The multiple weight loss steps indicate the presence of multiple components in the sample as well as its decomposition [28].

### **2.2.10.3 Differential Thermal Analysis (DTA)**

Differential thermal analysis (DTA) is a technique measuring the difference in temperature between a sample and a reference (a thermally inert material) as a function of the time or the temperature. The DTA method detects transformation for all categories of materials. The temperature difference between reference and sample is monitored as a function of temperature [29]. The area under the DTA peak is the change in enthalpy and is not affected by the heat capacity of the sample [29]. The DTA curve provides data on the glass transitions, crystallization, melting and sublimation. In addition, however, physical changes that do not involve weight changes can be detected by DTA. DTA thermal curves can be used to determine the order of a reaction (kinetics) and construct phase diagrams for materials. DTA can also be used for the characterization of engineering materials for the determination of the structural and

## [Chapter 2: Experimental Techniques and Characterization Methods]

---

chemical changes occurring during sintering, fusing, heat treatments of alloys to change microstructure, identification of different types of synthetic rubbers, and determination of structural changes in polymers. Fig. 2.19 (a) and (b) show the DTA instrument and its set-up respectively.

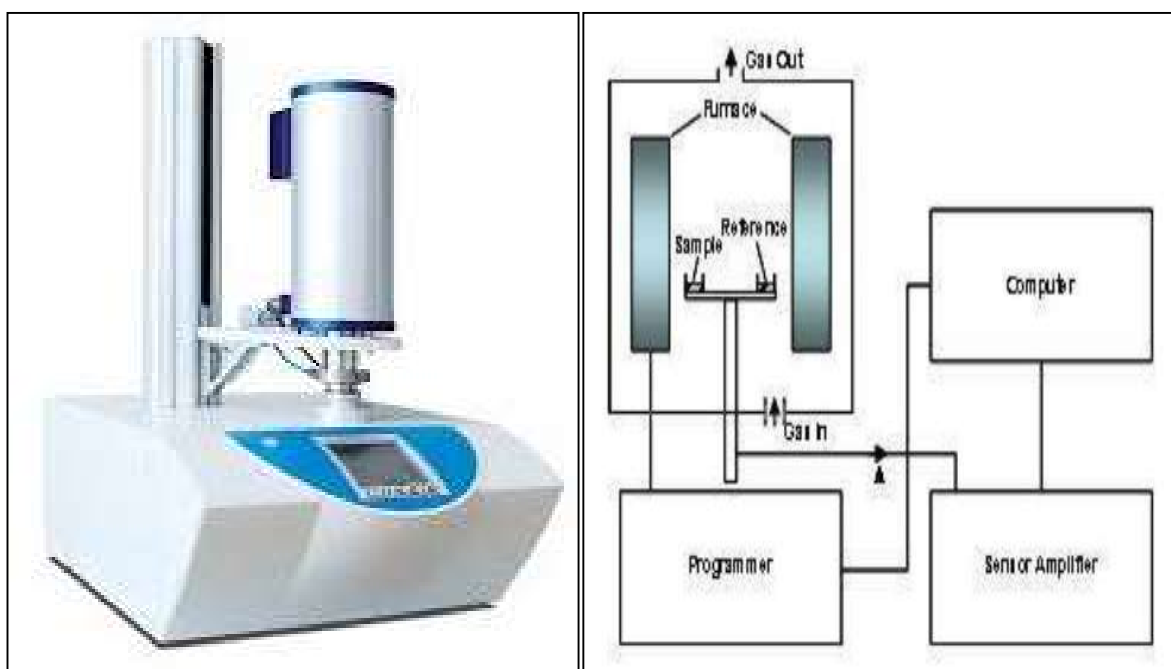


**Fig. 2.19:** (a) The Differential Thermal Analyzer and (b) Instrumental set-up of DTA.

The DTA consists of a sample holder, thermocouples, sample containers, ceramic or metallic block, a furnace, a temperature programmer and a recording system. The key feature is the existence of two thermocouples connected to a voltmeter. One thermocouple is placed in an inert material such as  $\text{Al}_2\text{O}_3$ , while the other is placed in a sample of the material under study. As the temperature increases the voltmeter will show a deflection if the sample undergoes a phase transition. This happens due to the fact that heat raises the temperature of the inert substance which in turn incorporates latent heat to change the phase of material.

## [Chapter 2: Experimental Techniques and Characterization Methods]

---

### References

1. E. M. Engler, Chem. Technol. 17, 542 (1987).
2. S. X. Dou, H. K. Liu, A.J. Bourdillon, J. P. Zhou, N. X. Tan, X. Y. Sun and C. C. Sorrell, J. Am. Ceram. Soc. 71C, 329 (1998).
3. C. J. Brinker and G. W. Scherer, "Sol-Gel Science" Academic Press Inc, Boston, 3, pp. 908 (1990).
4. D. Rana, "Dopant effect on the structural, electrical, magnetic and magneto transport properties of colossal magnetoresistancemanganites", Ph.D. thesis, Saurashtra University, Rajkot (2004).
5. A. R. West, Solid State Chemistry and its Applications, John Wiley and Sons, Chichester, New York, 20, pp. 492 (1984).
6. <http://www.mrl.ucsb.edu/mrl/centralfacilities/xray/xray-basics/index.html>
7. E. N. Kaufmann, "Characterization of Materials", 2<sup>nd</sup> edition, John Wiley and Sons 3, pp. 1392 (2003).
8. B. D. Cullity, "X-ray Diffraction" 3<sup>rd</sup> edition, Addison-Wesley, New York, 1, 555 (1972).
9. C. Kittel, "Introduction to Solid State Physics" John Wiley, New York, pp. 164 (1986).
10. B. D. Cullity, "Elements of X-Ray Diffraction" 2<sup>nd</sup> edition, Addison-Wesley Publishing Company, Inc. pp. 664 (1978).
11. R. Guinebretiere, X-ray Diffraction by Polycrystalline Materials, ISTE Ltd, Lavoisier pp. 351 (2006).
12. A. Monshi, M. R. Foroughi and M. R. Monshi, World J. Nano Sci. Eng. 2, 154 (2012).
13. H. M. Rietveld, J. Appl. Cryst. 2, 65 (1969).
14. N. Sahu and S. Panigrahi, Bull. Mater. Sci. 34, 1495 (2011).
15. H. M. Rietveld, J. Acta. Cryst. 22, 151 (1967).
16. J. I. Langford and D. Louer, Rep. Prog. Phys. 59, 131 (1996).
17. L. B. McCusker, R. B. Von Dreele, D. E. Cox, D. Louer and P. Scardi, J. Appl. Cryst. 32, 36 (1999).
18. F. Haguenu, P. W. Hawkes, J. L. Hutchison, B. Satiat Jeunemaître, G. T. Simon and D. B. Williams, Microsc. Microanal. 9, 96 (2003).

## [Chapter 2: Experimental Techniques and Characterization Methods]

---

19. G. Piccaluga, A. Corrias, G. Ennas and A. Musinu, Sol-gel preparation and characterization of Metal-Silica and Metal-Oxide silica nanocomposites, Mater. Sci. Foundation (Trans Tech Publication, Uetikon, Switzerland), 13, pp. 4 (2000).
20. R. L. Whetten, M. N. Shafiqullin, J. T. Koury, T. G. Schaaff and I. Vezmar, M. M. Alvarez and A. Wilkinson, Acc. Chem. Res. 32, 397 (1999).
21. J. I. Goldstein, D. E. Newbury, P. Echlin, D. C. Joy, C. Fiori and E. Lifshin, Scanning electron microscopy and X-ray Microanalysis, Springer, New York, pp. 673 (1981).
22. S. Foner, Rev. Sci. Instrum. 30, 548 (1959).
23. E. Verdonck, K. Schaap and L.C. Thomas, Int. J. Pharmaceutics 192, 3 (1999).
24. J. A. Dean, The Analytical Chemistry Handbook, McGraw Hill, New York, pp. 1168, (1995).
25. A. S. Douglas, F. J. Holler and T. Nieman, Principles of Instrumental Analysis, 5<sup>th</sup>ed. New York, pp. 805 (1998).
26. J. M. Barton, The application of differential scanning calorimetry (DSC) to the study of epoxy resin curing reactions. In: advances in Polymer Science, Springer, Berlin, Heidelberg, New York, Tokio, 72, pp. 111 (1985).
27. A. W. Coats and J. P. Redfern, Analyst 88, 906 (1963).
28. M. E. Brown and P. K. Gallagher, Handbook of Thermal Analysis and Calorimetry: Recent Advances, Techniques and Applications, Elsevier, Netherlands, 5, pp. 517 (2007).
29. H. K. D. H. Bhadeshia, "Thermal analysis techniques, Differential thermqal analysis", University of Cambridge, Material Science and Metallurgy, [www.msm.cam.ac.uk/phase-trans/2002/Thermal1.pdf](http://www.msm.cam.ac.uk/phase-trans/2002/Thermal1.pdf).